

# The role of adhesion in tapping-mode atomic force microscopy

D. Sarid, J.P. Hunt, R.K. Workman, X. Yao, C.A. Peterson

Optical Sciences Center, University of Arizona, Tucson AZ 85721, USA  
 (E-mail: sarid@sarid.opt-sci.arizona.edu)

Received: 25 July 1997/Accepted: 1 October 1997

**Abstract.** The equation of motion of the cantilever of an atomic force microscope (AFM) operating in the tapping mode in the presence of tip–sample adhesion modeled by the JKR theory is solved self-consistently. The vibration of the cantilever is discussed in terms of the parameters characterizing the properties of the cantilever, tip, and sample. A comparison with the experimental phase-shifts as a function of the setpoint reported by Magonov et al. is presented and sample indentation and tip–sample force and pressure are analyzed.

In an atomic force microscope (AFM) operating in the tapping mode, the position  $s_{\text{bm}}$  of the bimorph-mounted cantilever is slowly moved toward the sample as it is vibrated close to its resonance frequency [1]. Once the tip of the cantilever starts tapping the surface of the sample, its amplitude of vibration decreases and phase of oscillation shifts. The operator of the AFM will usually prescribe a certain setpoint, which is the ratio of the tapping amplitude to that of the freely vibrating cantilever. This ratio will be maintained by the AFM electronic feedback system. By raster scanning the tapping tip across the surface of the sample, one can obtain two surface maps: one of the position of the bimorph required to satisfy the setpoint, yielding the topography of the surface, and the other of the phase-shift that contains a rich body of information concerning the local elastic and adhesion properties of the surface [1–8]. To extract this information, it is imperative to know the instantaneous, local sample indentation as well as tip–sample force and pressure. Unfortunately, experimental methods to measure these three properties have yet to be devised. It is therefore of fundamental importance to have a self-consistent model that incorporates the key parameters of the tapping-mode system, and in particular adhesion, and compare the calculated phase-shifts as a function of the setpoint with experimental results.

In this paper we present such a self-consistent model incorporating the Johnson, Kendall, and Roberts (JKR) adhesion theory [9–11] in our previously developed AFM

tapping-mode model [12, 13]. The parameters used in this model consist of the spring constant of the cantilever  $k$ , average quality factor  $Q$ , amplitude and frequency of vibration of the driving bimorph  $a_{\text{bm}}$  and  $f$ , respectively, average tip position  $s_{\text{av}}$ , tip and sample radius  $R_i$ , Young's modulus  $E_i$ , Poisson's ratio  $\nu_i$ , and tip–sample Hamaker's constant  $A$ . We have used a set of parameters similar to those of a tapping-mode experiment reported by Magonov et al. and were able to reproduce their experimentally observed phase-shift as a function of the setpoint for two polyethylene samples. The agreement between theory and experiment, therefore, gives credence to the theoretically derived sample indentation and tip–sample force and pressure that shed light on the instantaneous tip–sample interaction.

The remainder of this paper is organized into three sections. Section 1 describes the JKR adhesion theory, Sect. 2 the self-consistent tapping-mode theory, and Sect. 3 the calculated results of the phase-shift, surface indentation, tip–sample force and pressure, and a discussion showing the important role that adhesion plays in tapping-mode AFM.

## 1 The JKR adhesion theory

Let the effective tip–sample radius of curvature  $R$  be defined by  $R = R_1 R_2 / (R_1 + R_2)$ . The Hertzian adhesion force  $F_{\text{H}}$  between two rigid spheres separated by a distance  $D \ll R$  is [11]

$$F_{\text{H}} = 2\pi R W_{1,2}(D). \quad (1)$$

Here  $W_{1,2}(D)$ , the work of adhesion, is the energy per unit area of two flat surfaces separated by  $D$ . The surface energy  $\gamma$  is related to the energy required to separate two flat surfaces from contact to infinity. It is given in terms of Hamaker's constant  $A$  by [11]

$$\gamma = \frac{W_{1,2}}{2} = \frac{A}{24\pi D_0^2}. \quad (2)$$

A rough approximation of  $D_0$  can be obtained by  $D_0 = \sigma/2.5$  where  $\sigma$  is a typical interatomic distance [11]. The Hertzian adhesion theory that treats rigid bodies has been extended to deformable bodies by Johnson, Kendall, and Roberts [9, 10]. Their theory is used here to find the functional dependence connecting the sample indentation and tip-sample radius of contact, contact force, and pressure.

The elastic modulus of two spheres representing the tip and sample is given by  $\kappa_i = (1 - \nu_i^2)/\pi E_i$ , where the effective elastic modulus is given by  $\kappa_{\text{eff}} = \kappa_1 + \kappa_2$ . The JKR theory yields the contact force,  $F$ , as a function of contact radius

$$F = -\sqrt{\frac{2k_s q r^3}{R}} + \frac{k_s r^3}{R}, \quad (3)$$

where  $q = 3\pi R W_{1,2}$ , and

$$k_s = \frac{4}{3\pi} \frac{1}{\kappa_{\text{eff}}}. \quad (4)$$

Note that for  $W_{1,2} = 0$  and in the absence of an external force the tip will rest on the surface of the sample, just “touching” it. However, for  $W_{1,2} > 0$  and in the absence of an external force the tip will embed itself inside the sample at such a depth that the attractive adhesion force equals the repulsive indentation force. The radius of contact  $r_0$  at this point is

$$r_0 = \left( \frac{6\pi R^2 W_{1,2}}{k} \right)^{1/3}. \quad (5)$$

One can now apply an external force to bring the embedded tip back to the surface of the sample. Pulling it farther away from this surface will result in the creation of a neck connecting the two. The neck will keep growing until the adhesion force can no longer sustain it, whereupon the neck breaks. The tip-sample attractive force at this point,  $F_s$ , is obtained by

$$F_s = -\frac{3\pi}{2} R W_{1,2}. \quad (6)$$

The radius of contact at separation,  $r_s$ , which is the radius of the “neck”, is

$$r_s = \frac{r_0}{4^{1/3}}. \quad (7)$$

The tip-sample indentation,  $d$ , as a function of the radius of contact  $r$  is

$$d = -\frac{r^2}{R} + \frac{2}{3} \frac{r_0^3}{R} r^{1/2}. \quad (8)$$

Note that a finite  $W_{1,2}$  increases the indentation for a given radius of contact. Also, the indentation can only be negative for a vanishing  $W_{1,2}$  whereas it can be negative or positive for a finite  $W_{1,2}$ . The tip-sample pressure at the center of the contact area  $P_c$  is

$$P_c = \frac{3k_s r}{2\pi R} - \sqrt{\frac{3k_s W_{1,2}}{2\pi r}}. \quad (9)$$

### 1.1 The Lennard–Jones potential

Let the tip-sample interaction,  $W_{\text{LJ}}(s)$ , be modeled as a Lennard–Jones potential given by

$$W_{\text{LJ}} = \left[ \frac{AR}{6\sigma} \right] \left[ \frac{1}{210} \left( \frac{\sigma}{s} \right)^7 - \frac{\sigma}{s} \right] \quad (10)$$

where  $s$  is the tip-sample distance. The first term on the right is the magnitude of the potential in terms of the product  $A R_{\text{tip}}$  and the second term describes its shape. The force  $F$ , which is obtained from the potential by taking the negative of its derivative, vanishes at  $s_0$ . We will therefore define the tip-sample indentation as  $d = s - s_0$ .

The total tip-sample force is obtained by combining the adhesion and Lennard–Jones forces in their respective regimes of applicability. The plot of the total force as a function of the tip-sample displacement will yield a hysteresis loop because the adhesion is not a single-valued function; it is quite different when the tip approaches the sample from a great distance and is then pushed into it, than when the tip is pulled out of the sample until it is separated from it.

## 2 The self-consistent tapping-mode theory

The equation of motion of the bimorph-driven cantilever is given by

$$\begin{aligned} \frac{\partial^2}{\partial t^2} s(t) + \frac{\omega_0}{Q} \frac{\partial}{\partial t} s(t) + \omega_0^2 [s(t) - s_{\text{bm}} - a_{\text{bm}} \sin(\omega t)] \\ = \frac{\omega_0^2}{k} F[s(t)] \end{aligned} \quad (11)$$

where  $f$  is the operating frequency,  $\omega_0 = 2\pi f_0$  the angular resonance frequency, and  $a_{\text{bm}}$  the bimorph amplitude of vibration [12–16]. It is important to note that, on resonance, only if the setpoint is less than 1 will the tip actually tap the surface. For larger values of the setpoint, the operation will be in the noncontact mode. Note also that the total force  $F[s(t)]$ , which is due to both adhesion and indentation, is a double-valued function of position. We can now solve the equation of motion self-consistently using typical experimental parameters.

## 3 Modeling results

The model presented in this paper has been used to calculate the cantilever displacement and velocity, surface indentation, tip-sample force and pressure, and phase-shift as a function of the setpoint. The parameters used in the calculation consisted of a spring constant of 40 N/m and a free cantilever amplitude of 100 nm [8]. Theoretical and experimental phase-shifts as a function of setpoint were in agreement when we used  $R_{\text{tip}} = 50$  nm,  $f = f_0 = 150$  kHz,  $Q = 100$ , and  $E_{\text{poly},1} = 0.2$  GPa and  $E_{\text{poly},2} = 0.033$  GPa for the rigid and compliant regions of the polyethylene sample, and  $A = 10^{-19}$  J. Note that for simplicity the model assumes that the tip of the cantilever is spherical rather than the apex of an inverted pyramid, and that Young’s modulus of the polyethylene sample is close to that reported in the literature.

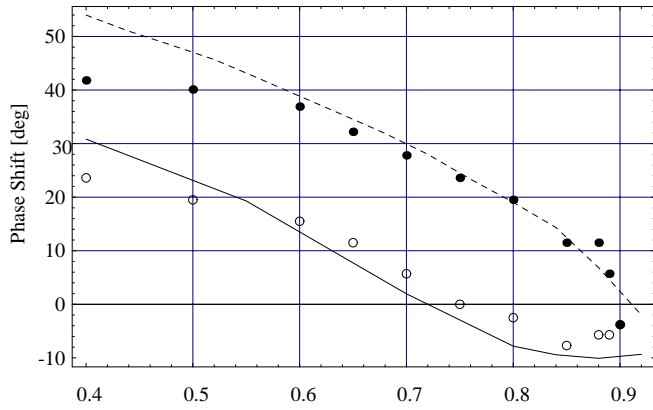
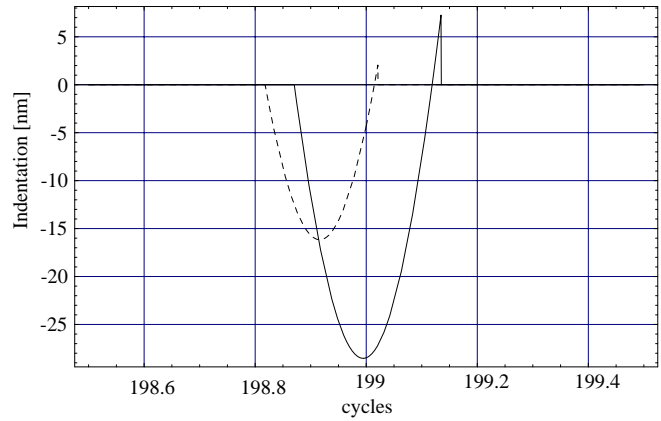


**Fig. 1.** The phase-shift as a function of setpoint for tapping on rigid (*solid circles*) and compliant (*open circles*) regions of the polyethylene sample; the *solid* and *dashed* lines are the respective calculated results

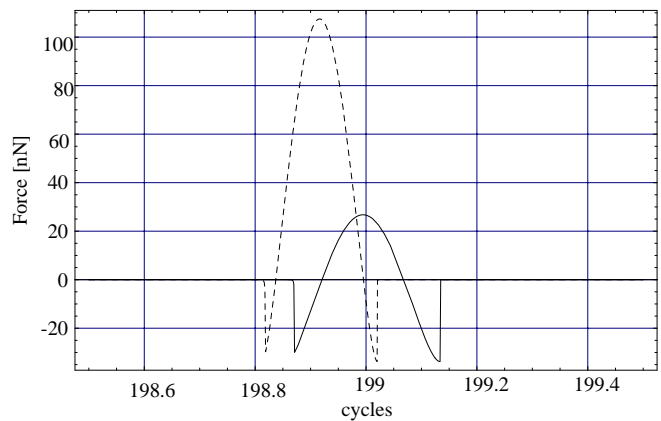
Figure 1 shows experimental and calculated phase-shifts as a function of setpoint. The solid and open circles represent the experimental results for tapping on rigid and compliant regions of the polyethylene sample, respectively. The dashed and solid lines are the respective calculated results. The good fit between theory and experiment leads to the conclusion that during the tapping process the tip experiences both attractive and repulsive forces, the former giving rise to a negative phase-shift and the latter to a positive phase-shift. The overall phase-shift will therefore consist of contributions from both repulsive and attractive regions of the tip-sample force curve. The most dramatic result observed in Fig. 1 is the important role adhesion plays in determining the net phase-shift; for a sufficiently large setpoint amplitude ratio and for a compliant enough sample, the attractive adhesion force is larger than the repulsive indentation force and the overall phase-shift is therefore negative. This behavior is observed in Fig. 1 for setpoints larger than 0.7 for the compliant material (solid line). For the more compliant regions, the repulsive force apparently dominates the tip-sample interaction. For a smaller setpoint, the repulsive indentation force is much larger than the attractive adhesion force for both samples, and the net phase-shift is positive. For a setpoint less than 0.5, the agreement between theory and experiment breaks down, requiring a refinement of the theory. Since the calculated phase-shift as a function of setpoint is found to agree with experiment, it is encouraging to continue further and explore the predicted sample indentation and tip-sample force and pressure using a typical setpoint of, say, 0.7.

Figure 2 shows the sample indentation as a function of time for the rigid (*dashed line*) and compliant (*solid line*) regions of a polyethylene sample where the maximum indentation, as expected, is larger on the compliant region of the sample. An important feature in this figure is the small positive indentation observed at the right-hand side of each indentation curve, representing the neck that forms between the sample and the tip as the latter is pulled out of the sample. The abrupt change from a positive to zero indentation demonstrates the growth of the neck until the adhesion can no longer sustain it whereupon it breaks.

Figure 3 shows the tip-sample force as a function of time where the force is considered positive when repulsive and negative when attractive. As expected, the rigid regions of



**Fig. 2.** The sample indentation as a function of time where the *solid* and *dashed lines* refer to the compliant and rigid regions of the sample, respectively



**Fig. 3.** The tip-sample force as a function of time where the *solid* and *dashed lines* refer to the compliant and rigid regions of the sample, respectively

the sample exert a greater repulsive force on the tip. The negative part of the force on the left-hand side of the peak represents the tip-sample interaction during which the tip is being pushed into the sample. It differs from the force at the right-hand side of the peak that represents the tip-sample interaction during which the tip is being pulled out of the sample. The right-hand side of the force curve is deeper and broader than it is at the left-hand side because of the formation of a neck between tip and sample. The force exerted by the tip on the sample is not a very important quantity since it does not tell us anything about the damage that it can inflict on the sample. Rather, it is the maximum tip-sample pressure which is of interest because it is this quantity that can damage both the tip and sample. We find that the maximum pressure exerted by the tip on the compliant regions of the sample is 14.1 MPa while for the rigid regions of the sample it is 73.7 MPa. Now hitting a rigid sample with a sharp tip is known to dull the tip or indent the sample inelastically, while the opposite is true for a compliant sample which is indented more. Although the pressure on a compliant sample is found to be smaller than on a rigid one, it is the mechanical strength of the sample that determines whether it will be damaged during the tapping process.

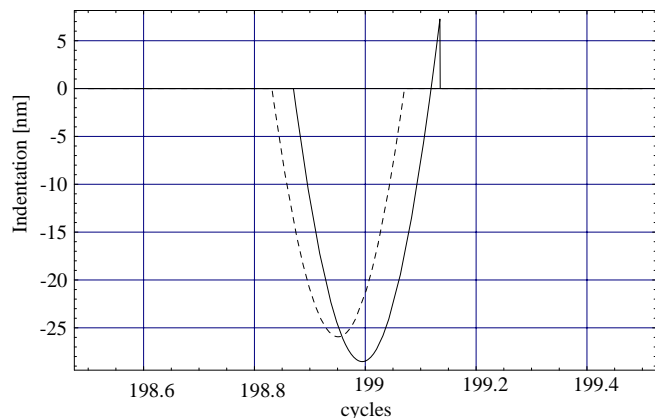


**Fig. 4.** The sample indentation as a function of time where the *solid* and *dashed* lines represent the theoretical results with and without adhesion taken into account, respectively

To appreciate the role of adhesion in the tapping process we present in Fig. 4 the indentation of the compliant regions of the sample when adhesion is considered (solid line) and when it is ignored (dashed line). Adhesion clearly adds to the maximum indentation and is responsible for the neck forming between the tip and sample. Adhesion also plays a role in the dependence of the phase-shift on the setpoint, as shown in Fig. 5 for a sample with  $E_{\text{poly}} = 0.1$  GPa and  $R = 25$  nm. Here the solid and dashed lines refer to the cases where adhesion is present or absent, respectively. Note that the presence of adhesion reduces the phase-shift when tapping on the compliant regions of the sample for a large setpoint, where it can even become it negative.

In conclusion, it was shown that including tip-sample adhesion in the model describing the operation of a tapping-mode AFM makes it possible to obtain agreement with experimental phase-shift as a function of setpoint. This agreement gives credibility to the calculated sample indentation and tip-sample force and pressure, which are important factors in analyzing surface phase-shift maps. It is important to note that although we used a macroscopic theory that is only an approximation to realistic tip-sample interactions, the results are expected to reproduce the salient features of this important surface characterization technology.

*Acknowledgements.* Support for this work was provided by the Center for Microcontamination Control (University of Arizona), the BMDO through the AASERT program, the Army Research Office, and Digital Instruments. The authors thank S.N. Magonov, V. Elings, and M.-H. Whangbo for allowing us to use their experimental results.

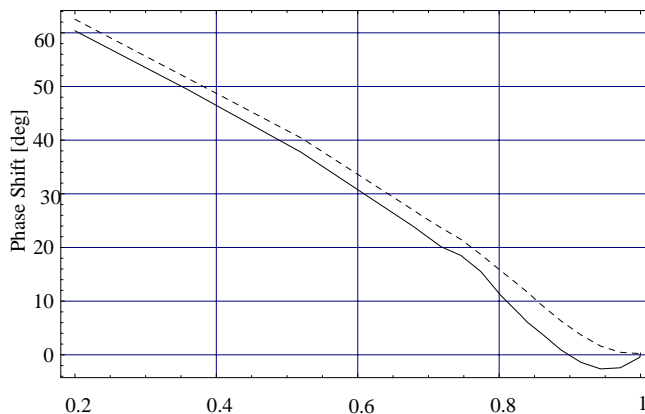


**Fig. 5.** The phase-shift as a function of the setpoint for  $a_{\text{bm}} Q = 100$  nm and  $E_{\text{poly}} = 0.1$  GPa. The *solid* and *dashed* lines represent the theoretical results with and without adhesion taken into account, respectively

## References

1. Q. Zhong, D. Inniss, K. Kjoller, V.B. Elings: *Surf. Sci. Lett.* **290**, L688 (1993)
2. H.G. Hansma, J.H. Hoh: *Annu. Rev. Biophys. Biomol. Struct.* **23**, 115 (1994)
3. P.K. Hansma, J.P. Cleveland, M. Radmacher, D.A. Walters, P.E. Hillner, M. Bezanilla, M. Fritz, D. Vie, H.G. Hansma, C.B. Prater, J. Massie, L. Fukunaga, J. Gurley, V. Elings: *Appl. Phys. Lett.* **64**, 1738 (1994)
4. C.A.J. Putman, K.O. Van der Werf, B.G. De Groot, N.K. van Hulst, J. Greve: *Appl. Phys. Lett.* **64**, 2454 (1994)
5. G.Y. Chen, R.J. Warmack: *J. Appl. Phys.* **78**, 1465 (1994)
6. J.P. Spatz, S. Sheiko, M. Moller, R.G. Winkler, P. Reineker, O. Marti: *Nanotechnology* **6**, 40 (1995)
7. B. Anczykowski, D. Kruger, H. Fuchs: *Phys. Rev. B* **53**, 15485 (1996)
8. S.N. Magonov, V. Elings, M.-H. Whangbo: *Surf. Sci.* **375**, L385 (1997)
9. K.L. Johnson, K. Kendall, A.D. Roberts: *Proc. R. Soc. London A* **324**, 301 (1971)
10. K. Kendall: *J. Phys. D: Appl. Phys.* **4**, 1186 (1971)
11. J. Israelachvili: *Intermolecular Forces* 2nd edn. (Academic Press, New York 1992)
12. J. Chen, R.K. Workman, D. Sarid, R.R. Höper: *Nanotechnology* **5**, 199 (1994);  
D. Sarid, J. Chen, R.K. Workman: *Comp. Mat. Sci.* **3**, 475 (1995);  
D. Sarid: *Comp. Mat. Sci.* **5**, 291 (1996);  
D. Sarid, T.G. Ruskell, R.K. Workman, D. Chen: *J. Vac. Sci. Technol.* **14**, 864 (1996)
13. D. Sarid: *Exploring Scanning Probe Microscopy with Mathematica* (Wiley, New York, 1997)
14. J. Tamayo, R. Garcia: *Langmuir* **12**, 4430 (1996)
15. D. Gruger, B. Anczykowski, H. Fuchs: *Ann. Phys.* **5**, 341 (1997)
16. N.A. Burnham, O.P. Behrend, F. Oulevey, G. Gremandi, P.J. Gallo, D. Gourdon, E. Dupas, A.J. Kulik, H.M. Pollock, G.A.D. Briggs: *Nanotechnology* **8**, 67 (1997)
17. D. Sarid, *Scanning Force Microscopy* (Oxford University Press, Oxford 1991) revised edn. (1994)